Recombination dynamics of luminescence in colloidal CdSe/ZnS quantum dots

2005 Nanotechnology 16 1517

(http://iopscience.iop.org/0957-4484/16/9/018)

INSTITUTE OF PHYSICS PUBLISHING NANOTECHNOLOGY
Nanotechnology **16** (2005) 1517–1521 doi:10.1088/0957-4484/16/9/018

Recombination dynamics of luminescence in colloidal CdSe/ZnS quantum dots

W Z Lee[1], G W Shu[1], J S Wang[1], J L Shen[1,7], C A Lin[2], W H Chang[2], R C Ruaan[3], W C Chou[4], C H Lu[5] and Y C Lee[6]

[1] Physics Department, Chung Yuan Christian University, Chung-Li, Taiwan, Republic of China
[2] Department of Biomedical Engineering, Chung Yuan Christian University, Chung-Li, Taiwan, Republic of China
[3] Department of Chemical and Material Engineering, National Central University, Chung-Li, Taiwan, Republic of China
[4] Electrophysics Department, National Chiao-Tung University, Hsin-Chu, Taiwan, Republic of China
[5] Department of Chemical Engineering, National Taiwan University, Taipei, Taiwan, Republic of China
[6] Department of Computer Science and Information Engineering, Tung Nan Institute of Technology, Taipei, Taiwan, Republic of China

E-mail: jlshen@cycu.edu.tw

Received 13 December 2004, in final form 25 May 2005
Published 29 June 2005
Online at stacks.iop.org/Nano/16/1517

Abstract

Recombination dynamics of photoluminescence (PL) in colloidal CdSe/ZnS quantum dots (QDs) were studied using time-resolved PL measurements. The PL intensity shows a biexponential decay at 9 K, consisting of a fast component (∼1 ns) and a slow component (∼6.3 ns). Based on the emission-energy and temperature dependence of carrier lifetimes, we suggest that the fast and slow PL decay of colloidal CdSe/ZnS QDs originates from recombination of the delocalized carriers in the internal core states and the localized carriers at the interface, respectively.

(Some figures in this article are in colour only in the electronic version)

1. Introduction

Semiconductor quantum dots (QDs) with dimensions on the length scale of a few nanometres provide a nearly zero-dimensional system, where carrier confinement occurs in all spatial directions. The quantum confinement results in the changes of the density of states for both electrons and phonons and the mechanisms of electron–hole recombination. The optical properties of semiconductor QDs are expected to exhibit high luminescence yield and thermal stability due to their δ-like density of states and strong quantum confinement [1]. The refractive index and nonlinear optical properties of semiconductor QDs change significantly compared to those of bulk [2]. Because of their novel optical properties, semiconductor QDs have led to considerable applications in optoelectronic devices such as optical switches, light-emitting diodes (LEDs), and lasers [1, 3, 4]. In recent years, colloidal semiconductor QDs have been coupled to biological molecules such as proteins and DNA [5–9]. These QD bioconjugates can be used as biomedical fluorescence labels for investigating biomolecular interactions and developing high-sensitivity detection and imaging [5–9]. One important concern in these applications is the dynamic properties of luminescence from QDs, which not only help to gain fundamental insight into the charge carrier properties but also provide information to improve the luminescence yield. The recombination dynamics of colloidal CdSe QDs has been studied recently [10–15]. The radiative lifetime of photoluminescence (PL) is generally dominated by a biexponential distribution, consisting of a fast component (∼several nanoseconds) and a slow component (∼tens of nanoseconds) at room temperature. However, origins of the fast and slow decays of PL in colloidal CdSe QDs are not conclusive in previous studies. Based on a delayed rise in

---

[7] Author to whom any correspondence should be addressed.

0957-4484/05/091517+05$30.00

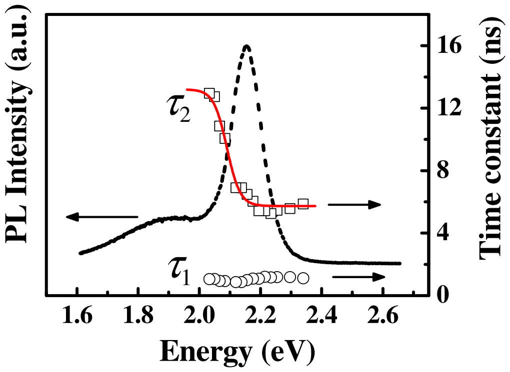

Figure 1. The PL intensity of colloidal CdSe/ZnS QDs at 9 K (dashed line). The open circles and squares show mission energy dependence of τ_1 and τ_2, respectively. The solid line displays the calculated τ_2 using equation (2).

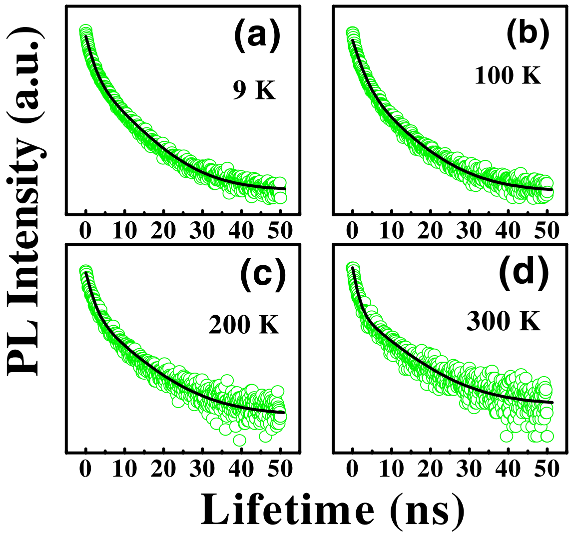

Figure 2. The PL decay profiles of colloidal CdSe/ZnS QDs monitored at bandgap transition (2.153 eV) at temperatures between 9 and 300 K. The solid lines display the result calculated using equation (1).

luminescence that is consistent with the population of traps, Landes *et al* suggested that both shorter and longer lifetimes of PL decay occur from trap states, not directly from the band-edge states [11]. Wang *et al* attributed the shorter and longer lifetimes of PL to the intrinsic recombination of initially populated core states and the involvement of surface states, respectively [12, 13]. On the other hand, Javier *et al* pointed out that a photoinduced charged exciton and an intrinsic band-edge exciton is responsible for the shorter and longer lifetime of PL decay, respectively [14]. Obviously, the origin of PL decays in colloidal CdSe QDs remains an open question.

It is well known that the time-resolved PL, using the kinetics of electron–hole recombination as a probe, gives direct information on the luminescence decay mechanism. In this study, we investigate the recombination dynamics of colloidal CdSe QDs based on the results of time-resolved PL measurements. The PL intensity at 9 K shows a biexponential decay, consisting of a fast component (~1 ns) and a slow component (~6.3 ns). Based on the emission energy and temperature dependence of the lifetimes, we suggest that the fast and slow decay involves recombination of the delocalized carriers and the localized carriers, respectively.

2. Experimental details

The investigated colloidal core/shell CdSe/ZnS QDs were synthesized by the following procedure. 0.30 g of cadmium oxide (CdO), 1.30 g of tetradecylphosphonic acid (TDPA) and 25.0 g of tri-*n*-octylphosphine oxide (TOPO) were loaded into a 250 ml flask and heated to 320 °C under argon flow. After CdO was totally dissolved in TDPA and TOPO, the temperature of the solution was cooled to 300 °C and a 4.45 ml of selenium stock solution (a 0.5 M of selenium solution in tributylphosphine, TOP) was injected. The mixture was then followed by the dropwise addition of 1.5 ml of precursor solution (made by mixing 1.75 ml of $ZnMe_2$ (2.0 M in toluene) and $S(Si(CH_3))_2$ in TBP) to cover a layer of a higher bandgap semiconductor, ZnS. After the mixture was cooled down to room temperature, QDs were precipitated by adding methanol. The precipitate was washed by methanol several times with centrifugation and the CdSe/ZnS core/shell QDs were obtained after drying under vacuum. To synthesize the carboxylated QDs, a 20 mg of TOP/TOPO capped CdSe/ZnS QDs was mixed with a 200 mg 11-mercaptoundecanoic acid (MUA) in a reaction vessel. Methanol was added and the pH value was adjusted to about 10 with tetramethylammonium hydroxide. The mixture was heated under reflux for 2 h. After cooling to room temperature, the resulting water-soluble QDs were precipitated with tetrahydrofuran and separated by centrifugation.

PL time-resolved measurements were performed using the technique of time-correlated single-photon counting (TCSPC). The PL measurements were obtained using a pulsed GaN diode laser operating at a wavelength of 396 nm as the excitation source. The diode laser produces light pulses with 50 ps duration and a repetition rate of 1 MHz. The sample was mounted in a closed-cycle helium cryostat, at temperatures between $T = 9$ and 300 K. The collected luminescence was directly projected into a grating spectrometer and detected with a high-speed photomultiplier tube (PMT). The PL signal is fed into a TimeHarp counting card, which was triggered with a signal from the diode laser. The instrument response of this time-correlated single-photon counting system is about 300 ps.

3. Results and discussion

The dashed line in figure 1 displays the PL signal of colloidal CdSe/ZnS QDs at 9 K. The energy of the main peak is centred at 2.153 eV, which is assigned to the recombination of near-bandgap excitons. The broad peak around 1.85 eV is attributed to the deep trap emission from mid-gap states that arise from surface defects or un-passivated surface atoms [16]. Figure 2(a) displays the PL decay profile of CdSe/ZnS QDs monitored at the peak of the near bandgap transition (2.153 eV). The decay can be well fitted by a biexponential function:

$$I(t) = A_1 e^{-\frac{t}{\tau_1}} + A_2 e^{-\frac{t}{\tau_2}}, \qquad (1)$$

where τ_1 (τ_2) represents the decay time of fast (slow) decay; A_1 (A_2) represents the amplitude of the fast-decay (slow-decay) component at $t = 0$. The solid line in figure 2(a) shows the fitted result, which is in good agreement with experimental result. The decay curve gives time constants of $\tau_1 = 0.98$ ns for the fast decay and $\tau_2 = 6.3$ ns for the slow decay. It is known that Auger recombination can be a non-radiative pathway for carrier relaxation and lead to non-exponential relaxation. In the case of Auger recombination one electron–hole pair recombines and transfers all of its energy to a third particle as additional kinetic energy. Since Auger recombination is a three-body collision, the average number of electron–hole pairs created in each QD was estimated to verify whether the non-exponential relaxation involves Auger recombination. With the average pump power of ~ 0.1 mW cm^{-2} in our experiments, it was found that less than one electron–hole pair would be injected into a QD. Additionally, the lifetime of Auger recombination was predicted to decrease as the temperature increases [17]. We shall see below that the lifetimes of PL decay in CdSe/ZnS QDs increase as the temperature increases from 9 to 200 K. These features suggest that Auger recombination should be ruled out from the interpretation of PL decay here.

To investigate the origins of τ_1 and τ_2, PL decay profiles were analysed by the emission energy dependence. The open circles and squares in figure 1 show the measured lifetimes for different emission energy. As shown in figure 1, the lifetimes of fast PL decay (τ_1) remain unchanged with increasing emission energy; however, the lifetime of slow PL decay τ_2 decreases, which is a characteristic of the localization process of excitons [18]. The localization of electrons or holes may be generated at the heterointerface of QDs due to interface roughness, or interface defects [10]. In the exciton transfer model, localized carriers can transfer from higher energy sites to lower energy sites through a relaxation process [19]. The decay rate of localized carriers is expressed as the radiative recombination rate plus the transfer rate to lower energy sites. Thus, the observed lifetime decreases as the emission energy increases. The combination of recombination and transfer has been modelled by assuming the density of localized tail states is proportional to $\exp(-E/E_0)$, where E_0 describes the amount of spreading in the density of states [19, 20]. The relationship between lifetime $\tau(E)$ and PL energy E is the function [20]

$$\tau(E) = \frac{\tau_{\mathrm{rad}}}{1 + \exp[(E - E_{\mathrm{me}})/E_0]}, \tag{2}$$

where τ_{rad} is the radiative lifetime, E_{me} is defined by a definite energy for which the decay time equals the transfer time, and E_0 is the depth of the localized states. τ_2 described by equation (2) is plotted with a solid line in figure 1. A good fit to experiment confirms the existence of carrier localization. We therefore suggest that there are two distinctly different kinds of state in QDs, the slow-decay component of PL is originated from the recombination of carriers from the localized states, and the fast-decay component of PL is associated with the recombination of carriers from the delocalized states. From the fitting curve based on the exciton localization model, τ_{rad}, E_{me}, and E_0 are estimated to be 13.2 ns, 2.1 eV, and 22 meV, respectively. E_{me} is the energy similar to the mobility edge. In our case, above 2.1 eV the transfer of excitons has a higher probability than the radiative decay. E_0 is a measure of average localization energy of the QDs. This energy can also be examined in relation to the temperature dependence of slow PL decay. This will be discussed later in the text.

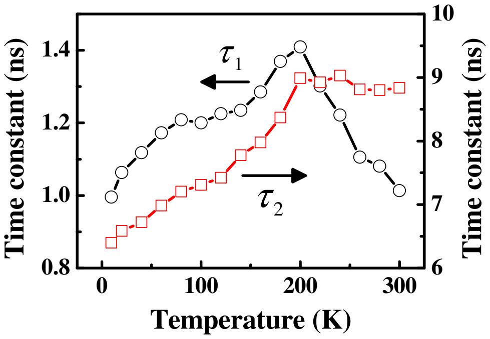

Figure 3. The temperature dependence of the PL decay times in colloidal CdSe/ZnS QDs. The lines are guides to the eye.

Figures 2(b), (c), and (d) display the PL decay profiles of CdSe/ZnS QDs at 100, 200, and 300 K, respectively. The decay profiles in figures 2(b)–(d) were again fitted by the biexponential function, as shown in the solid lines, and the decay lifetimes (τ_1 and τ_2) can be also obtained according to the fits. The effect of temperature upon the lifetimes (τ_1 and τ_2) is shown in figure 3. It is found that τ_1 and τ_2 increase at temperatures below 200 K. Recently, the temperature-dependent exciton lifetime in CdSe QDs has been studied by Crooker *et al* [21]. In their studies, the exciton lifetimes are consistent with a picture of thermal activation of excitons from the dark ground state [21]. However, the exciton lifetimes in their studies ($\sim$20–900 ns) are much longer than the lifetimes we investigate here. The increased lifetime with temperature has been observed in self-assembly QDs previously [22, 23]. This behaviour has been explained by exciton dissociation at elevated temperature and escape of carriers into the wetting layer, leading to a subsequent recapture in another QD. The recapture results in the population of carriers in QDs being replenished and the increase of PL decay time at higher temperatures. However, this explanation cannot be applied to the experimental result in figure 3 since there is no wetting layer in our colloidal QDs. We suggest that the increase of the decay times at higher temperatures is probably due to a finite spatial phase-coherence effect [24, 25]. According to Citrin's calculation, the spatial coherence of excitons in QDs produces a mixing of large-wavevector states which are nonradiative into the small-wavevector radiative states, thus increasing the radiative lifetimes compared with the quasi-two-dimensional system [25]. As the temperature increases, a larger number of excited states of the centre-of-mass motion are occupied and the radiative lifetimes increases further. This explains the increase of τ_1 and τ_2 as temperature increases. The spatial coherence model expects lifetimes of the QDs with smaller coherence area to extrapolate to a larger lifetime at zero temperature. In figure 3, the extrapolated intercept is about 0.95 and 6.2 ns for τ_1 and τ_2, respectively. The larger intercept for τ_2, which is associated with the smaller coherence area (localized states), can thus be accounted for by the coherence-area argument. At higher temperatures ($T > 200$ K), τ_1

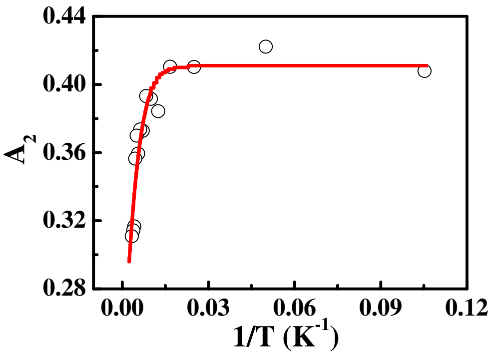

Figure 4. The amplitudes of slow decay of PL in colloidal CdSe/ZnS QDs (A_2) as a function of the reciprocal temperature. The solid lines display the result calculated using equation (3).

decreases above 200 K, while τ_2 remains nearly unchanged up to 300 K. The decrease of τ_1 with increasing temperature, accompanied by a pronounced decrease of the PL intensity (not shown), is attributed to predominance of nonradiative recombination due to thermal activation. Since the temperature independence of τ_2 occurs in parallel with the decrease of τ_1, the constant τ_2 can be explained by the thermal escape of carriers from the internal core states to interface localized states, leading to the population of the localized states to be replenished at high temperatures.

The open circles in figure 4 show the amplitudes of slow decay (A_2) as a function of the reciprocal temperature. It is found that A_2 remains unchanged at temperatures below ~50 K and decreases at higher temperatures. To extract an activation energy, we fit A_2 to the form

$$A(T) = A_0/[1 + C\exp(-E_A/kT)], \qquad (3)$$

where E_A is the activation energy and C is a fitting constant. The solid line in figure 4 is the calculated result according to equation (3). A fit to the data yields $E_A = 26$ meV, which is in agreement with the depth of the localized states E_0 (22 meV), obtained from equation (2). As the temperature increases, the excitons become delocalized from the localized states, leading to the decrease of A_2 accordingly. Thus, the spatial localization of excitons is further supported by the behaviour of the amplitudes of slow decay as a function of the temperature. Figure 5 displays the PL decay profile of CdSe/ZnS QDs monitored at deep-trap emission (1.85 eV) at 9 K. The decay curve was empirically fitted by a single exponential function. The solid line in figure 5 shows the fitted result, which gives a time constant of 5.4 ns for the mono-exponential decay. This relaxation time is different from the fast decay time (τ_1) of near bandgap emission; however, it is roughly close to the slow decay time (τ_2) of near bandgap emission. This can be understood by the fact that the untrapped exciton (delocalized exciton) emission is basically absent in this energy range and only the recombination of the trapped carriers is observed.

4. Summary

In summary, we study recombination dynamics of colloidal CdSe/ZnS QDs using time-resolved PL. The decay of PL intensity at 9 K can be best fitted by a biexponential function, indicating a fast component (~1 ns) and a slow component (~6.3 ns). Based on the emission energy and temperature dependence of the lifetimes, we suggest that the fast and slow PL decay involves recombination of the delocalized states in the core region and the localized states at the heterointerface of the QDs, respectively.

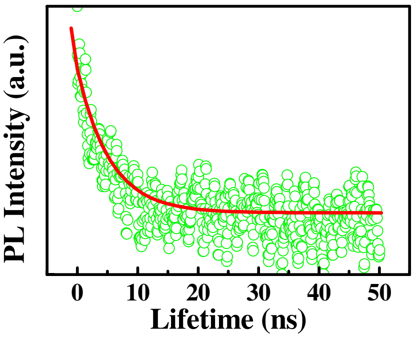

Figure 5. The PL decay profiles of colloidal CdSe/ZnS QDs monitored at deep-trap emission (1.85 eV) at 9 K.

Our experimental studies on the luminescence decay time confirmed that the interfacial properties play a crucial role in the optical properties of semiconductor QDs. This work is expected to be useful to clarify the mechanism of luminescence in colloidal CdSe/ZnS QDs and hence increase the quantum yield for luminescence. Understanding optical properties in colloidal CdSe/ZnS QDs may make them particularly useful for further development of light emission diodes, lasers, quantum computers, bio-labels and bioanalytical applications.

Acknowledgments

This project was supported in part by the National Science Council under grant numbers 93-2112-M-033-010 and NSC 93-2120-M-033-001.

References

[1] Bimberg D, Grundmann M and Ledentsov N N 1998 *Quantum Dot Heterostructures* (New York: Wiley)
[2] Schmitt-Rink S, Miller D A B and Chemla D S 1987 *Phys. Rev.* **35** 8113
[3] Collier C P, Vossmeyer T and Heath J R 1998 *Annu. Rev. Phys. Chem.* **49** 371
[4] Coe S, Woo W K, Bawendi M and Bulović V 2002 *Nature* **420** 800
[5] Bruchez M Jr, Moronne M, Gin P and Weiss S 1998 *Science* **281** 2013
[6] Chan W C W and Nie S M 1998 *Science* **281** 2016
[7] Mattoussi H, Mauro J M, Goldman E R, Anderson G P, Sundar V C, Mikulec F V and Bawendi M G 2000 *J. Am. Chem. Soc.* **122** 12142
[8] Mitchell G P, Mirkin C A and Letsinger R L 1999 *J. Am. Chem. Soc.* **121** 8122
[9] Pathak S, Choi S K, Arnheim N and Thompson M E 2001 *J. Am. Chem. Soc.* **123** 4103
[10] Chen X, Lou Y, Samia A S and Burda C 2003 *Nano Lett.* **3** 799
[11] Landes C, Burda C and El-Sayed M A 2001 *J. Phys. Chem.* B **105** 2981

[12] Wang X, Qu L, Zhang J, Peng X and Xiao M 2003 *Nano Lett.* **3** 1103
[13] Wang X, Zhang J, Nazzal A, Darragh M and Xiao M 2002 *Appl. Phys. Lett.* **81** 4829
[14] Javier A, Magana D, Jennings T and Strouse G F 2003 *Appl. Phys. Lett.* **83** 1423
[15] Hines M A and Guyot-Sionnes P 1996 *J. Phys. Chem.* **100** 468
[16] Cordero S R, Carson P J, Estabrook R A, Strouse G F and Buratto S K 2000 *J. Phys. Chem.* B **104** 12137
[17] Pankove J I 1973 *Optical Processes in Semiconductors* (New York: Dover)
[18] Passow T *et al* 2002 *J. Appl. Phys.* **92** 6546
[19] Cohn E and Sturge M D 1982 *Phys. Rev.* B **25** 3828
[20] Strassburg M, Dworzak M, Born H, Heitz R, Hoffmann A, Barteis M, Lischka K, Schikora D and Christen J 2002 *Appl. Phys. Lett.* **80** 473
[21] Crooker S A, Barrick T, Hollingsworth J A and Klimov V I 2003 *Appl. Phys. Lett.* **82** 2793
[22] Yu H, Lycett S, Roberts C and Murray R 1996 *Appl. Phys. Lett.* **69** 4087
[23] Yang W, Lowe-Webb R R, Lee H and Sercel P C 1997 *Phys. Rev.* B **56** 13314
[24] Citrin D S 1992 *Phys. Rev. Lett.* **69** 3393
[25] Citrin D S 1993 *Supperlatt. Microstruct.* **13** 303